

Chapter III

ESTIMATES OF UPWELLING RATES IN THE ARABIAN SEA

The Arabian Sea, a part of the northern Indian Ocean regime, is known for its seasonally reversing summer and winter monsoonal wind patterns and associated upwelling and convective mixing (Wyrski, 1971, 1973; Shetye et al., 1994). These processes result in the well-known seasonal oscillation in the biological productivity of these waters (Qasim, 1977, 1982; Lal, 1994; Krishnaswami and Nair, 1996). The upwelling and biological productivity is expected to influence the air-sea exchange of CO₂ and its budget in the atmosphere. A large body of its intermediate water (~200-1000 m) remains suboxic throughout the year, and there is perennial denitrification (Naqvi, 1991). Detailed measurements of various chemical and biological parameters have been made in the Arabian Sea to determine air-sea exchange fluxes of CO₂ during the Indian Joint Global Ocean Flux Study (George et al., 1994; Krishnaswami and Nair, 1996; Sarma et al., 1998).

The phenomenon of upwelling in the Indian Ocean is unique with an absence of equatorial upwelling unlike in the Pacific and the Atlantic Ocean. This is because the Southeast Trades do not cross the equator preventing equatorial divergence responsible for upwelling (Schott and McCreary, 2001). The upwelling in the Indian Ocean is confined to coastal areas north of the equator. This upwelling leads to an upward migration of deep (greater than 50 m), cool, nutrient rich ¹⁴C depleted waters to the surface resulting in enhanced productivity.

Radiocarbon (^{14}C) is a useful tracer, for studies of ocean circulation and pathways of carbon across various exchangeable carbon reservoirs (Broecker et al., 1985). Cosmic ray produced ^{14}C in the atmosphere is now an established geochronometer and is used widely for various archeological and geological date estimation. The atmospheric ^{14}C levels nearly doubled due to injection of considerable amounts of ^{14}C in the environment by nuclear weapon tests conducted during the late 1950s and early 1960s (Nydal and Lovseth, 1983;

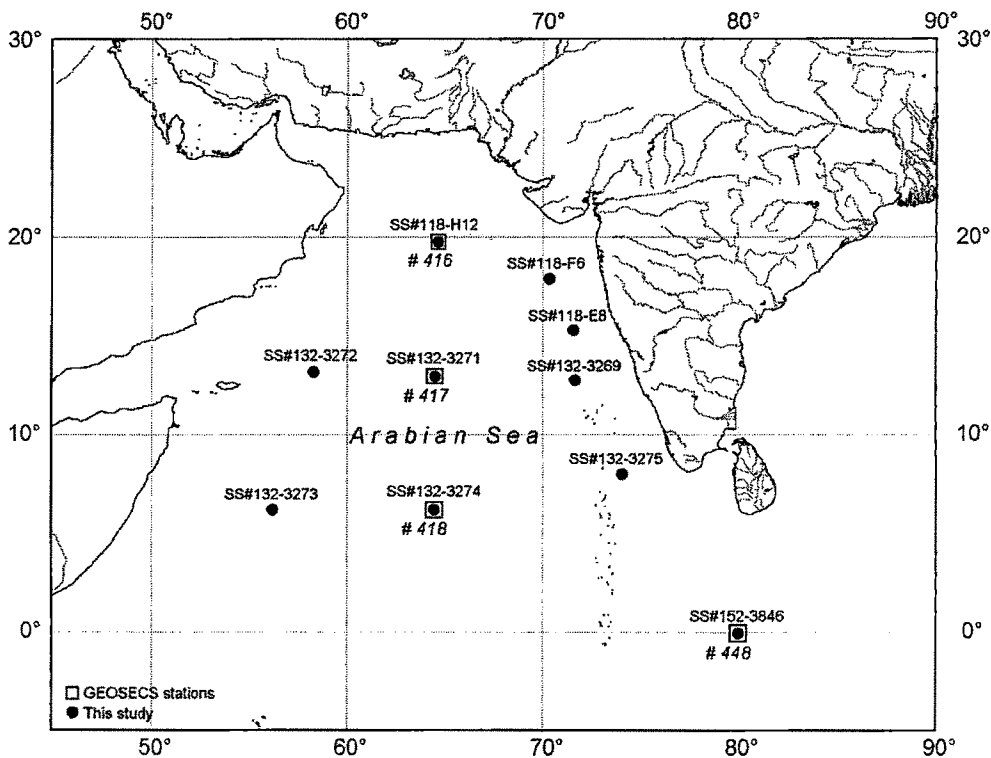


Fig. 3.1: Location of sampling stations in the Arabian Sea. The boxed filled circles are the GEOSECS stations occupied during this study almost after two decades

Broecker and Peng, 1994). This transient of bomb ^{14}C in the environment during early 1960s gave an opportunity to study circulation pattern in the upper water column of oceans and the exchange of CO_2 at the air-sea interface—processes that take place in decadal time scales (Lassey et al., 1990). The earliest ^{14}C measurements in the water column of the Arabian Sea and Indian Ocean were made between 1977-'78, as part of the GEOSECS expedition (Stuiver and Ostlund, 1983).

Several stations in the Arabian Sea and the equatorial Indian ocean were occupied for sampling the water column during the 1994 to 1995 period in various cruises onboard FORV *Sagar Sampada* (Fig. 3.1). Nearly ten samples per profile, from pre-selected depths were collected for ^{14}C analysis. Onboard measurements of nutrients, dissolved inorganic carbon (ΣCO_2) as well as processing for ^{14}C analysis were done on these samples.

Determination of bomb ^{14}C inventory and air-sea CO_2 exchange rates

Knowledge of the inventory of bomb ^{14}C in the sea and its distribution provides useful information on the ventilation in the upper ocean and the air-sea exchange of CO_2 . ^{14}C that has been measured in the water column since the mid-1950s is made of two components, natural (i.e., cosmic ray-produced) and that injected via bomb tests (bomb ^{14}C). Thus, to obtain the inventory of bomb ^{14}C from the measured ^{14}C activity in these waters, accounting for contributions from natural ^{14}C is necessary. Data on pre-bomb ^{14}C profiles in seawater, particularly in the Indian Ocean, are sparse, and hence indirect approaches have been used to derive these profiles in the upper ocean areas using suitable proxies.

To obtain the pre-bomb ^{14}C distribution in the thermocline, various methods have been used. The first method proposed by Broecker et al. (1985) relies on the use of $\Delta^{14}\text{C}$ values of surface waters measured prior to nuclear weapon tests and an estimate made for the penetration depth of bomb ^{14}C based on the vertical distribution of ^3H introduced in the ocean via weapon tests. Available data on ^{14}C in surface waters sampled before 1957 and on corals and shells deposited prior to nuclear weapon tests have been used as pre-bomb $\Delta^{14}\text{C}$ values for surface seawater. There are no measurements of ^{14}C in the Arabian Sea waters prior to the weapon tests. The only available data for pre-bomb ^{14}C in the region are from the measurements of corals in the Gulf of Kutch; 22.6°N, 70°E, a coastal region in the northeastern Arabian Sea (Chakraborty, 1993). The $\Delta^{14}\text{C}$ in a coral sample formed during the 2 year

period between 1949 and 1951, is $-60 \pm 5\%$ (this measurement was made by homogenizing the coral sample deposited during the 2 year period). This, however, compares well with the values of -60 to -65% used by Broecker et al. (1985) in their model for calculating bomb ^{14}C inventory in the Indian Ocean. In this work, a value of -60 to -65% has been used for pre-bomb Arabian Sea surface water $\Delta^{14}\text{C}$. During GEOSECS, ^3H (tritium) measurements were made to determine the penetration depth of bomb ^{14}C (Ostlund et al., 1980; Stuiver, 1980; Broecker et al., 1985). In this study, however, tritium could not be measured as its concentration in water has decreased significantly since the GEOSECS through radioactive decay ($t_{1/2}=12.3$ years) and by mixing during the intervening ~ 2 decades. The bomb ^{14}C inventory in stations H-12, 3271, and 3274 (reoccupation of GEOSECS 416, 417, and 418 respectively) were, however, calculated using the pre-bomb ^{14}C profiles simulated using the GEOSECS tritium data.

In the second method, Broecker et al. (1995) and Peng et al. (1998) have used the correlation between $\Delta^{14}\text{C}$ and dissolved silica in waters deeper than 1000 m (waters devoid of ^3H) to derive pre-bomb ^{14}C profiles in the thermocline. In this study, pre-bomb ^{14}C profiles were simulated using the silica analogy ($\Delta^{14}\text{C} = -70 - \text{SiO}_2$ ($\mu\text{M kg}^{-1}$)) (Broecker et al., 1985) using GEOSECS silica data and forcing the surface water $\Delta^{14}\text{C}$ to be in the range of -60 to -65% , as determined from pre-bomb coral samples from the Gulf of Kutch. These profiles form the basis to estimate the bomb ^{14}C component from the measured ^{14}C profiles (regression analysis of SiO_2 versus $\Delta^{14}\text{C}$ data from the Arabian Sea and the Bay of Bengal waters collected during GEOSECS having $\text{SiO}_2 > 50 \mu\text{M kg}^{-1}$) yield a relation of $\Delta^{14}\text{C} = -80 - 0.83\text{SiO}_2$ ($\mu\text{M kg}^{-1}$). The pre-bomb $\Delta^{14}\text{C}$ profiles based on this relation and those derived using Broecker et al. (1995) method are consistent within $\pm 10\%$. Considering this, the Broecker et al. (1995) relation has been used as its intercept is closer to the measured $\Delta^{14}\text{C}$ in pre-bomb corals. In addition, the bomb ^{14}C inventories for these two stations were calculated based on pre-

bomb ^{14}C profiles derived from all the GEOSECS stations in the Arabian Sea (GEOSECS stations 413, 416, 417, 418, and 419). The results show that all the inventories calculated are within $\pm 10\%$. This comparison suggests that the uncertainties introduced in the calculation of bomb ^{14}C inventories, by assuming that pre-bomb ^{14}C profiles in stations from the same latitudinal belt are the same, is unlikely to be more than $\pm 10\%$.

The surface $\Delta^{14}\text{C}$ values, however, show a decrease in 1994–1995 values as compared to 1977–1978. This decrease can be attributed to a cumulative effect of low bomb ^{14}C input from the atmosphere and the vertical mixing in the upper water column. Rhein et al. (1997) observed that the penetration depth of CFC, another transient tracer introduced into the environment predominantly during mid 1900s is ~ 1000 – 1200 m in the Arabian Sea. The mean depth of bomb ^{14}C distribution (Z) (Broecker et al., 1985) in the present study ranged from 218 to 387 m. (In this discussion, Z , the mean depth of the bomb ^{14}C distribution, does not refer to the depth at which bomb ^{14}C can be detected; see Broecker et al. (1985) and the discussion below). The penetration depths of bomb ^{14}C (the depths to which bomb ^{14}C is discernible) as seen from the plots of $\Delta^{14}\text{C}$ versus depth is in the range of 800–1000 m (Fig. 3.2). At the GEOSECS stations 416, 417, and 418, Z increased by ~ 15 – 45% averaging $\sim 25\%$ over ~ 2 decades, from 1977 to 1995.

The bomb ^{14}C inventory is calculated using the relation

$$\Sigma^{14}\text{C} = K [Z \times \Sigma\text{CO}_2 \times (\Delta^{14}\text{C} - \Delta^{14}\text{C}^0)] \quad (1)$$

where, $\Sigma^{14}\text{C}$ = Bomb ^{14}C inventory in atoms cm^{-2} ;

ΣCO_2 = mean ΣCO_2 of the water column containing
bomb ^{14}C ($\mu\text{M kg}^{-1}$);

$$\Delta^{14}\text{C} = \delta^{14}\text{C} - 2(\delta^{13}\text{C} + 25) (1 + \delta^{14}\text{C}/1000)$$

(Stuiver and Polach, 1977);

Z = mean depth of bomb ^{14}C penetration (meters);

$\Delta^{14}\text{C}^0$ = pre-bomb surface water $\Delta^{14}\text{C}$ (-60 to -65‰);

$$= \frac{\text{Area}}{(\Delta^{14}\text{C} - \Delta^{14}\text{C}^o)}$$

Area = area under the curve between measured and pre-bomb ^{14}C profiles;

K is proportionality constant including various conversion factors (such as density, Avogadro's number, and $^{14}\text{C}/\text{C}$ abundance ratio).

Details of exchange rates calculations described by Bhushan et al. (2000) have been revised in this study, following Dutta (2001). ^{14}C concentration in the upper 1000 m

of the ocean is a mixture of natural and bomb components. Its measurements in the water column represents sum of the ^{14}C contributions from these two sources but to delineate the bomb ^{14}C component, it is necessary to have precise estimates of pre-bomb ^{14}C activity (i.e. natural ^{14}C)

in these waters. This requirement, however, is not fulfilled in several areas of the ocean including the Arabian Sea and Bay of Bengal as no measurements of ^{14}C were made in these areas during early 1950s. Therefore, indirect approaches based on the distribution of their proxies are used to derive the pre-bomb ^{14}C profile in the upper ocean. Based on bomb ^{14}C inventories, the air-sea CO_2 exchange rates (E) were calculated using the model of Stuiver (1980). The exchange rates are calculated assuming that the observed inventory of bomb ^{14}C is only due to the integrated gradient of ^{14}C between the atmosphere and oceanic mixed layer, with no lateral transport of ^{14}C . The

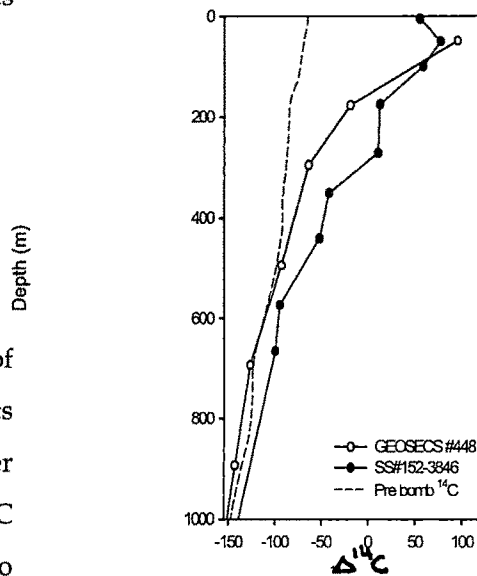


Fig. 3.2: Radiocarbon distribution in the upper 1000 m water column at the equatorial Indian Ocean station 3846. Also, shown the ^{14}C profile of GEOSECS for the station occupied during 1978. Dashed line is the pre-bomb ^{14}C simulated curve.

values of the integrals for $\Delta^{14}\text{C}_{\text{atm}}$ and $\Delta^{14}\text{C}_{\text{mix}}$ are obtained from ^{14}C measurements in the atmosphere and from corals respectively (Chakraborty et al., 1994). The input function of atmospheric ^{14}C used here is based on a model curve, constrained by atmospheric ^{14}C measurements at Israel, Ethiopia and Madagascar between 1963 and 1978 (Nydal and Lovseth, 1983, 1996), tree-ring ^{14}C measurements at Thane, India, near the Arabian Sea coast (Chakraborty et al., 1994), and atmospheric ^{14}C measurements over the Northern Indian Ocean between 1993 and 1997 (Bhushan et al., 1997; Dutta et

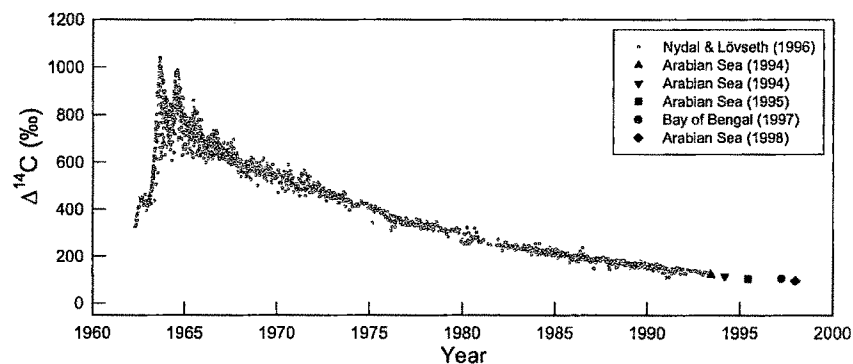


Fig. 3.3 Model $\Delta^{14}\text{C}$ of tropospheric CO_2 for the atmosphere over the Northern Indian Ocean used in the upwelling calculation (thick gray line). Tropospheric $\Delta^{14}\text{C}$ of Northern Hemisphere Zone 3 (Hua and Barbetti, 2004) is shown as thin line. Tropospheric $\Delta^{14}\text{C}$ values measured over the Arabian Sea during 1993-'95 and over the Bay of Bengal during 1997 (Dutta et al., 2006) are shown as filled circles.

al., 2006). The model atmospheric ^{14}C curve rose from 0‰ in 1954, peaking at 730‰ in 1964, and reducing to 570‰ in 1968. From 1968 onwards, an exponentially decreasing atmospheric $\Delta^{14}\text{C}$ trend with an e-folding time (removal time scale of ^{14}C from the atmosphere) of 17 years has been calculated fixing the $\Delta^{14}\text{C}$ for the years 1980 and 1999 at 265‰ and 88‰ respectively. The model atmospheric ^{14}C function is shown in Fig. 3.3, where it is compared with atmospheric ^{14}C compilations as made by Hua and Barbetti (2004) corresponding to the latitudes of the Arabian Sea and the north of equatorial Indian Ocean ("Northern Hemisphere Zone 3"). The integrated

values of atmospheric ^{14}C between 1954 and 1997 of these two curves differ by about 1%, which is not significant as compared to other uncertainties. The overall uncertainty for air-sea CO_2 exchange rates from bomb ^{14}C profiles is about $\pm 15\%$.

Determination of upwelling rates using 1-D model

In this study, upwelling rates are calculated based on the CO_2 exchange rates using a one dimensional (1-D) box diffusion model (Oeschger et al., 1975; Broecker et al., 1978). For this model calculation, the upper 1000 m of the water column is subdivided into 40 boxes, each 25 m thickness with the assumption that ^{14}C concentration within each of these boxes is homogeneous and that the top 100 m is well mixed. The model simulates the bomb ^{14}C depth profile with the defined CO_2 exchange rate (E), upwelling rate (w) and the vertical eddy diffusivity (K) for a given input function of bomb ^{14}C from atmosphere to the ocean surface layer. The same atmospheric ^{14}C input function is used as described in the previous section. The vertical eddy diffusivity (K) and the upwelling rate (w) were varied to generate ^{14}C depth profiles and the values that provided the best fit to the observed bomb ^{14}C profile were chosen as the mixing parameters for the station location. The best fit values of K range from 0.4 to 0.7 $\text{cm}^2 \text{sec}^{-1}$. In this study, the CO_2 exchange rates (E), as calculated earlier from bomb ^{14}C inventories for each station, have been used (Bhushan et al., 2000; Dutta 2001). However, for some stations, different exchange rates were used to obtain the best fit to observed bomb ^{14}C profiles.

Bomb ^{14}C inventory and air-sea CO_2 exchange rates

The bomb ^{14}C inventory in the Arabian Sea as estimated in this study ranges between $3\text{-}8 \times 10^9$ atoms cm^{-2} (Table 3.1). A relatively large bomb ^{14}C inventory of 8.0×10^9 atoms cm^{-2} was obtained at SS#132-3273 and at the equatorial Indian Ocean station SS#152-3846, the inventory has been 9.5×10^9 atoms cm^{-2} . Lower inventories at other locations in the northern Indian Ocean could have resulted either because of weak diffusive gas exchange leading to

low ^{14}C input or processes favouring vertical penetration (viz. wind speed) which, however, are not vigorous. It is known that on an average the wind speed over the Arabian Sea is $\sim 5 \text{ m s}^{-1}$ (Esbensen and Kushnir, 1981), which is less than the global average value.

Table 3.1: Upwelling rates based on bomb ^{14}C inventory for the Arabian Sea and the Equatorial Indian Ocean stations

Station	Location	Sampling date	Bomb ^{14}C Inventory $\times 10^9$ (atoms cm^{-2})	Air-sea CO_2 Exchange Rate (E) ($\text{mol m}^{-2} \text{ yr}^{-1}$)	Eddy diffusivity (K) ($\text{cm}^2 \text{ sec}^{-1}$)	Upwelling velocity (w) (m yr^{-1})
<i>Arabian Sea</i>						
SS#118-H-12	19.8°N; 64.6°E	Mar 1994	5.9	12.6	0.7	5
GEOSECS #416	-do-	Dec 1977	6.3	15.4	0.7	7
SS#118-F-6	17.9°N ; 70.3°E	Mar 1994	5.2	11.1	0.7	3
SS#118-E-8	15.3°N ; 71.5°E	Mar 1994	3.5	7.5	0.5	5
SS#132-3272	13.2°N ; 58.3°E	May 1995	6.4	13.7	0.5	4
SS#132-3271	13°N ; 64.5°E	Apr 1995	6.9	14.8	0.4	6
GEOSECS #417	-do-	Jan 1978	5.2	12.7	0.4	9
SS#132-3269	12.8°N ; 71.6°E	Apr 1995	4.8	10.3	0.5	4
SS#132-3275	8°N ; 74°E	May 1995	5.0	10.7	0.5	5
SS#132-3274	6.2°N ; 64.4°E	May 1995	6.4	13.7	0.4	5
GEOSECS #418	-do-	Jan 1978	6.1	15.0	0.4	9
SS#132-3273	5.7°N ; 56.2°E	May 1995	8.0	17.1	0.5	5
<i>Equatorial Indian Ocean</i>						
SS#152-3846	0°N ; 80°E	Mar 1997	9.5	20.4	0.4	5
GEOSECS #448	-do-	Apr 1978	5.0	12.1	0.4	5

The increase in bomb ^{14}C inventories at the Arabian Sea stations during the period between the GEOSECS expeditions and the present study is consistent with the model predictions of Toggweiler et al. (1989b). The increase in inventories are $\leq 30\%$ as compared to GEOSECS, and these are however, expected considering the significantly low $\Delta^{14}\text{C}$ values of the atmosphere since the GEOSECS expedition (Table 3.1).

The station SS#152-3846, reoccupation of the GEOSECS 448, at the equatorial Indian Ocean shows an increase in bomb ^{14}C inventory of ~95%, which could be a result of lateral transport of ^{14}C enriched waters. Bard et al. (1988, 1990) observed ~10-90% increase in the bomb ^{14}C inventory after about a decade of GEOSECS at some of the stations near the equatorial northwestern Indian Ocean. They attributed this increase to the advection of low salinity waters enriched in ^{14}C from the Indonesian through-flow along the equator to the 10°S latitudinal belt.

The CO_2 exchange rates for the Arabian Sea and the equatorial Indian Ocean are in the range of $7.5\text{-}20.4 \text{ mol m}^{-2} \text{ yr}^{-1}$, and are well within $\pm 30\%$ of the rates derived from the GEOSECS data (Table 3.1). Also, the gas exchange rates, computed using wind speeds, (Wanninkhof, 1992; Wanninkhof et al., 1985) are similar. Toggweiler et al. (1989b) computed CO_2 gas exchange rates for various oceanic regions based on a wind speed dependent model, wherein the exchange rates for the Arabian Sea were computed as $10\text{-}15 \text{ mol m}^{-2} \text{ yr}^{-1}$, with the highest values near the Somali Basin, a region known for the highest wind speeds and exceptionally strong wind induced upwelling. The exchange rates derived in this study from temporal variation of bomb ^{14}C inventory (Table 3.1) are in good agreement with predicted values (Toggweiler et al., 1989a). In the Arabian Sea, the highest exchange rate of $17.1 \text{ mol m}^{-2} \text{ yr}^{-1}$ was obtained for the station SS#132-3273, that is close to the Somali Basin value. The highest exchange rate as obtained for SS#152-3846 could be due to lateral inputs of ^{14}C enriched waters from the Indonesian through-flow along the equator.

Upwelling Rates

The upwelling rates determined for the Arabian Sea and equatorial Indian Ocean stations ranged from $3\text{-}9 \text{ m yr}^{-1}$ (Table 3.1). In general, it is noticed that the upwelling rates calculated for the stations occupied under this study are lower as compared to the GEOSECS stations. All the GEOSECS stations (416, 417 and 418 except for 448) have higher upwelling rates

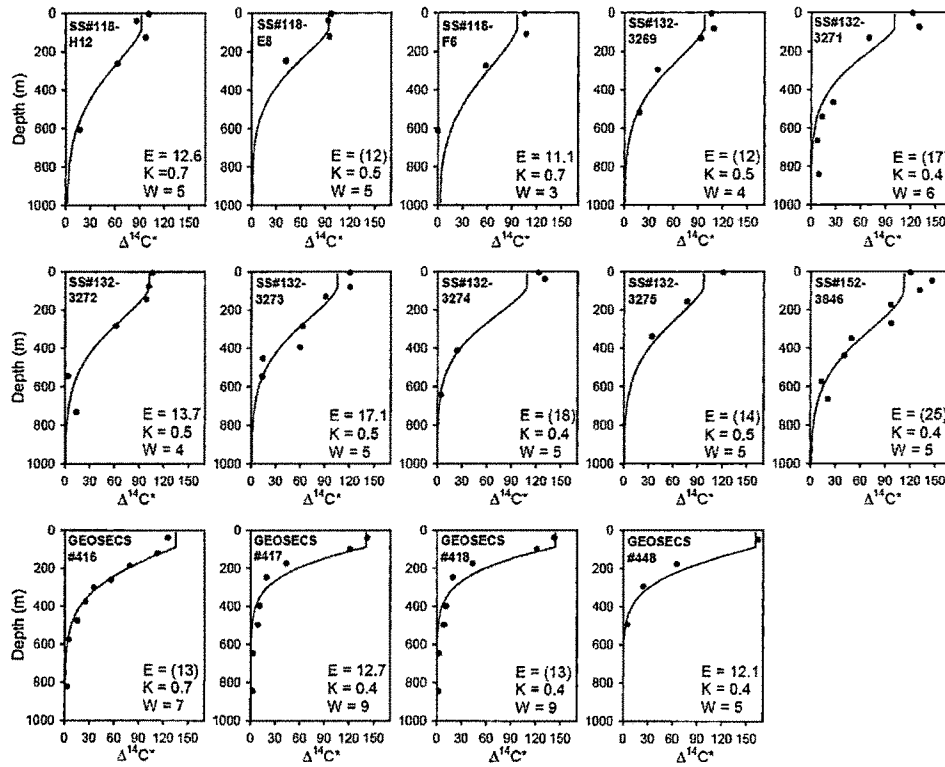


Fig. 3.4: Distribution of $\Delta^{14}\text{C}^*$ (excess bomb ^{14}C) versus depth for different stations. The solid line represents the simulated curve based on 1-D model of Oeschger et al., (1975) for the exchange rate (E), eddy diffusivity (K) and upwelling velocity (w).

compared to that observed for the same stations during this study after a period of nearly two decades (Fig. 3.4). However, GEOSECS station 448 and its reoccupation station SS#152–3846 show similar upwelling rates, with use of higher exchange rate for station SS#152–3846 (Fig. 3.4). As expected, the western region of the Arabian Sea that is known for high wind induced upwelling shows higher upwelling rate (Bhushan et al., 2008).

The difference in bomb ^{14}C inventory from the GEOSECS program (1977–1978) and this study (1994–1995) is in the range of $0.4\text{--}1.3 \times 10^9$ atoms cm^{-2} and are, not wholly inconsistent with the model predictions. Thus, the upwelling rates as derived from this study show values lower than expected. The upwelling rates as deduced from this study may be underestimates as this model does not take into consideration the horizontal advection of ^{14}C along the adjoining isopycnal surfaces. The upwelling rate estimation is

dependent on the gradient of bomb ^{14}C in the water column. This gradient is controlled by the atmospheric ^{14}C concentration, its penetration due to vertical mixing and the air-sea exchange rate and upwelling. The atmospheric ^{14}C concentrations during GEOSECS studies in the Indian Ocean (1977-78) are almost three times higher as compared to the present study (1994-94). As mentioned earlier the Trade winds do not cross the equator thereby inhibiting equatorial divergence that is responsible for the upwelling (Schott and McCreary, 2001). The upwelling in the equatorial region of the Indian Ocean is weak or negligible along the east coast of Kenya (Grumet et al., 2002a). The net result of upwelling is upward advection of relatively depleted $\Delta^{14}\text{C}$ waters enriched in nutrients to the surface thereby causing enhanced productivity. Generally, the surface ocean is depleted in $\Delta^{14}\text{C}$ compared to the atmospheric $\Delta^{14}\text{C}$ due to reservoir mixing time. With atmospheric excess of $\Delta^{14}\text{C}$, there is always an uptake of $\Delta^{14}\text{C}$ enriched CO_2 by the oceans. These processes lead to a vertical gradient of $\Delta^{14}\text{C}$ in the water column as a result of vertical mixing. Since radiocarbon is a transient tracer, the surface water concentrations are expected to have gradients which are time variant (Grumet et al., 2002b). With decreasing atmospheric ^{14}C concentrations, the vertical gradient in the water column ^{14}C distribution is expected to be modulated. This is responsible for the difference in upwelling rate estimates during two different time periods with such vast atmospheric $\Delta^{14}\text{C}$ differences. Although, during GEOSECS period, radiocarbon was more appropriate tracer due to its large air-sea $\Delta^{14}\text{C}$ gradient, however, during the present study it has yielded lower upwelling rates due to reduced water column $\Delta^{14}\text{C}$ gradient caused due to decreasing atmospheric $\Delta^{14}\text{C}$ (Rengarajan et al., 2002). The bomb ^{14}C introduction in the atmosphere proved to be a valuable tracer in understanding many surface processes of the oceans but it is limited by its removal from the atmosphere.